Analysis of models for the synapse between the inner hair cell and the auditory nerve

Xuedong Zhang
Hearing Research Center and Department of Biomedical Engineering, Boston University, Boston, Massachusetts 02215

Laurel H. Carney[a)]
Departments of Biomedical and Chemical Engineering and Electrical Engineering and Computer Science, Institute for Sensory Research, Syracuse University, Syracuse, New York 13244

(Received 4 September 2004; revised 9 June 2005; accepted 14 June 2005)

A general mathematical approach was proposed to study phenomenological models of the inner-hair-cell and auditory-nerve (AN) synapse complex. Two models (Meddis, 1986; Westerman and Smith, 1988) were studied using this unified approach. The responses of both models to a constant-intensity stimulus were described mathematically, and the relationship between model parameters and response characteristics was investigated. The mathematical descriptions of the two models were essentially equivalent despite their structural differences. This analytical approach was used to study the effects of adaptation characteristics on model parameters and of model parameters on adaptation characteristics. The results provided insights into these models and the underlying biophysical processing. This analytical method was also used to study offset adaptation, and it was found that the offset adaptation of both models was limited by the models' structures. A modified version of the synapse model, which has the same onset adaptation but improved offset adaptation, is proposed here. This modified synapse model produces more physiologically realistic offset adaptation and also enhances the modulation gain of model AN fiber responses, consistent with AN physiology. © *2005 Acoustical Society of America.* [DOI: 10.1121/1.1993148]

PACS number(s): 43.64.Bt [WPS] Pages: 1540–1553

I. INTRODUCTION

The inner-hair-cell (IHC) and auditory-nerve (AN) complex is a critical element in the peripheral auditory system that converts a mechanical signal (the response of the cochlea to sound) into a neural signal. Physiological studies (Westerman and Smith, 1984; Rhode and Smith, 1985; Westerman, 1985) have provided insight into the temporal dynamics of IHC-AN synaptic processing. The response of an AN fiber to a constant-intensity tone burst is typified by very rapid firing at the onset that declines with time, rapidly at first and then more slowly over a period of tens of milliseconds. The AN response after the offset of the stimulus (cessation of the stimulus) is greatly reduced relative to the spontaneous response and slowly recovers over several tens of milliseconds (Harris and Dallos, 1979; Westerman, 1985). Since the amplitude of the receptor potential of the IHC produced by a constant-amplitude stimulus (for example, a high-frequency tone) is essentially constant (Russell and Sellick, 1978), adaptation is believed to occur at the level of the transmitter release process in the IHC-AN synapse. Recent physiological studies (Moser and Beutner, 2000) provide direct evidence for the idea of adaptation at the IHC-AN synapse. The adaptation process in the IHC-AN synapse results in greater sensitivity to transient stimuli than to steady-state stimuli and underlies other temporal aspects of AN responses. These properties also limit some aspects of temporal coding of stimulus envelopes. For example, offset adaptation may be responsible in part for the psychophysical phenomenon of forward masking (Harris and Dallos, 1979).

IHC-AN synaptic adaptation is very complex. Its characteristics depend on stimulus intensity, duration, and previous stimulation history. Synaptic adaptation (Fig. 1) (Harris and Dallos, 1979) at the onset of AN responses to tone bursts is usually characterized functionally by two exponential components (Westerman and Smith, 1984; Rhode and Smith, 1985; Westerman, 1985):

$$R_{\text{on}}(t) = A_{\text{sus}} + A_r e^{-t/\tau_R} + A_{\text{st}} e^{-t/\tau_{\text{ST}}}, \tag{1}$$

where A_r and A_{st} are the components of rapid and short-term adaptation, τ_R and τ_{ST} are the respective decay time constants, and A_{sus} is a steady-state component. Adaptation at the offset of the stimulus can also be described as an exponential recovery component, with a different time constant than the onset, after a "deadtime" period, or a period of very low probability of firing:

$$R_{\text{off}}(t) = \begin{cases} 0; & t < t_0 \\ A_{\text{sp}}(1 - e^{-(t-t_0)/\tau_{\text{sp}}}) \end{cases}, \tag{2}$$

where A_{sp} is the spontaneous rate, t_0 is the deadtime period, and τ_{SP} is the recovery time constant of the offset responses. Other measurements that have helped characterize AN adaptation processes include responses to increments or decrements in stimulus intensity with an ongoing tonal background (Smith and Zwislocki, 1975;

[a)]Author to whom correspondence should be addressed; electronic mail: lacarney@syr.edu

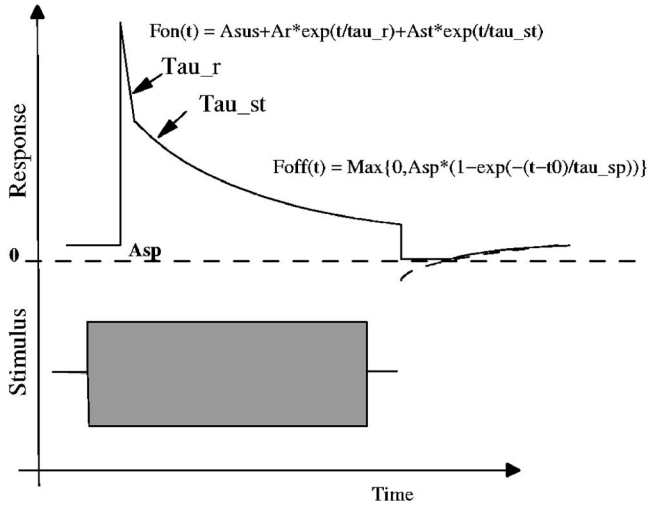

FIG. 1. Schematic diagram of the response of an AN fiber to a toneburst (Harris and Dallos, 1979; Westerman, 1985). The onset response of the AN fiber can be described as a sum of two exponential components [see Eq. (1)], and the offset response can be fit with a single exponential recovery function after a deadtime [Eq. (2)].

Smith *et al.*, 1985). Adaptation characteristics also differ for fiber types with different spontaneous rates (Rhode and Smith, 1985). The diversity and complexity of IHC-AN synaptic adaptation provide a challenge for the successful modeling of synapse dynamics (Hewitt and Meddis, 1991).

The mechanisms that give rise to synaptic adaptation can be due either to the depletion of a readily released presynaptic pool of neurotransmitter (Moser and Beutner, 2000) or the desensitization of the postsynaptic receptors (Raman *et al.*, 1994). The adaptation at IHC-AN synapse has often been modeled using multiple reservoirs of a neurotransmitter, with diffusion out of the cell and between reservoirs within the cell (Furukawa and Matsuura, 1978; Schwid and Geisler, 1982; Smith and Brachman, 1982; Meddis, 1986; Westerman and Smith, 1988; Ross, 1996). Each diffusion step is controlled by a permeability parameter, and at least one of the permeabilities in these models is determined by the stimulus (presumed to be controlled by IHC calcium concentration, intracellular IHC voltage, or equivalently, stimulus intensity). Adaptation of the synaptic output in these models depends on the reduction of the driving force for the diffusion of the synaptic material (transmitter) from the cell into the synaptic cleft (Fig. 2). Mathematically, low-pass filters are used to implement the replenishment and diffusion mechanisms between different transmitter reservoirs. These models can be implemented using either a cascade of low-pass filters or parallel low-pass filters, depending on the interconnection of the reservoirs.

The variation of adaptation characteristics across AN fibers makes it desirable to have different sets of model parameters to predict individual AN fiber responses more accurately, but determining these parameters is tedious. Compared to analytical solutions, the exhaustive search of a multidimensional parameter space using numerical methods is very time consuming, and the parameters may be trapped by local minima in the cost function. In addition, simulation

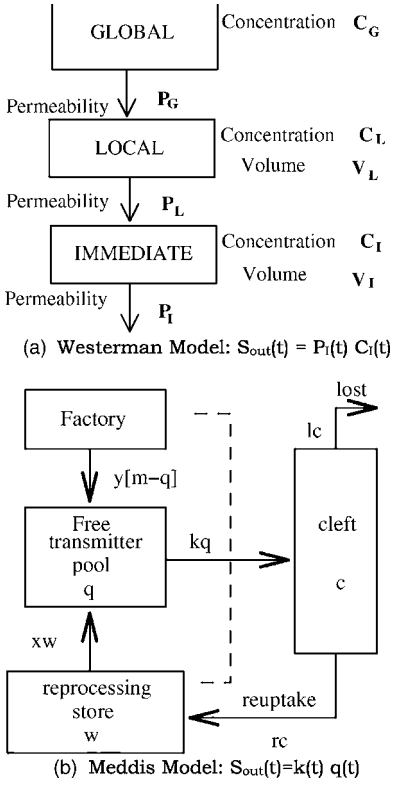

FIG. 2. Schematic diagram of two synapse models (Meddis, 1988; Westerman and Smith, 1988). (a) In the Westerman model [see Eqs. (6) and (7)], three transmitter reservoirs are cascaded, each with their own concentration and volume. The transmitter diffuses from global to local and then from local to immediate reservoirs. The output of the synapse model, S_{out}, is determined by the product of the concentration in the immediate reservoir and the diffusion permeability from the immediate reservoir into the synaptic cleft. (b) In the Meddis model [Eqs. (3)–(5)], the transmitter in the cleft is either lost or reprocessed by the reprocessing store (w). The free transmitter pool receives the transmitter from the reprocessing store or from a global factory and releases the transmitter into the cleft (c) with instantaneous release probability density k. The model synapse output is proportional to the amount of transmitter left in cleft (Meddis, 1988) or the rate of transmitter released into the cleft (Sumner *et al.*, 2002).

results may not give insight into a particular model; that is, quantitative relationships between the model parameters and adaptation properties may not be revealed by the exercise of fitting the parameters to a single fiber response, and the difference between different models may not be fully understood.

During the past twenty years, two IHC-AN synapse models with different structures have been developed independently and actively in a series of studies (Meddis, 1986, 1988; Westerman and Smith, 1988; Meddis *et al.*, 1990; Carney, 1993; Zhang *et al.*, 2001; Sumner *et al.*, 2002). Both of these models are very successful in simulating the onset adaptation responses of the AN fibers to some extent. For the model proposed by Westerman and Smith (1988), equations were derived to determine the model parameters from the desired shape of the onset of the peri-stimulus time (PST) histogram. A recent study (Zhang *et al.*, 2001) detailed how these parameters can be derived for different types of AN fibers. For the model proposed by Meddis (1986), the analytical relationship between steady-state responses and model parameters was described in a later study (Meddis *et*

al., 1990). This model was further explored in a recent study (Sumner *et al.*, 2002) to simulate the rate-level functions of low-, medium-, and high-spontaneous-rate AN fibers by changing parameters in the transmitter-release control function (that is, the stage that determines how the model IHC voltage affects the transmitter release permeability in the adaptation model) and synapse model parameters. However, the studies of other model adaptation characteristics (e.g., amplitudes and time constants of adaptation components) are limited by the sets of parameters provided by the authors (e.g., Hewitt and Meddis, 1991; Sumner *et al.*, 2002), which makes it difficult to understand the relationship between these parameters and different adaptation properties. Also, the difference in adaptation responses for these models, and whether the difference is a result of the different model structures or the different model parameter values, have not been clarified.

In this article, we use a unified approach to consider two models, that of Meddis (1986) and of Westerman and Smith (1988) (we will refer to the latter as the Westerman model). Since the essential architecture of the synapse model under investigation (interconnection of the synaptic reservoirs) has not been changed in the newer versions of these models (Zhang *et al.*, 2001; Sumner *et al.*, 2002), the results from this study are also applicable and beneficial to understanding the more recent versions of these models (see Sec. VI). In our approach, both models can be described as circuits of interconnected low-pass filters. In this framework, the responses of each model to a constant-intensity stimulus can be determined analytically, and relationships between the response characteristics and model parameters can be established. This mathematical method clarifies the differences and similarities between the two models, leading us to the conclusion that, despite their different structures, the two models are essentially the same. In addition, because the model equations provide better insight into the model structure, we can easily derive the model parameters on the basis of the desired adaptation properties.

There has been less attention paid to the modeling of offset adaptation at the IHC-AN synapse. It is difficult to find a common physiological explanation for both onset and offset adaptation because of the difference in their respective characteristic functions. Simulation results from models (Sumner *et al.*, 2003) have also not provided insights concerning the relationship between onset and offset adaptation.

We use our analytical approach to study the relationship between onset and offset adaptation in the Westerman and Meddis models. The model response characteristic function of offset adaptation is the same as that of onset adaptation, and is limited by the model parameters used to specify the desired onset adaptation. A modification for both models is then proposed; the modified model has the same onset adaptation but improved offset adaptation. The onset and offset adaptation responses are based on same physiological assumption in this modification. The modified offset adaptation enhances the modulation gain of the model AN fiber responses to modulated stimuli, consistent with AN physiology (Joris and Yin, 1992).

II. PHYSIOLOGICAL INTERPRETATION OF THE MEDDIS AND WESTERMAN SYNAPSE MODELS

In this section, we provide our physiological interpretation of the two models and explain how onset adaptation is achieved in both models. The similarities and differences between the two models are compared qualitatively here; their underlying physiological assumptions are further discussed in Sec. VI.

The model proposed by Meddis (1986, 1988) has three neurotransmitter reservoirs that are specified by the number of synaptic transmitters in the reservoir and arranged in a cycle: The immediate store (q); the synaptic cleft (c); and the reprocessing store (w) (see Fig. 2). New transmitter in the immediate store is either manufactured from the factory at a rate of $y[M-q(t)]$, where M is the amount of neurotransmitter in the global store), provided by a reprocessing store [at a rate of $xw(t)$], or released from the immediate store into the synaptic cleft at a rate of $k(t)q(t)$. The transmitter in the cleft is either lost at a rate of $lc(t)$ or recycled at a rate of $rc(t)$. The transmitter replenishment and release in the model can be described by the following equations:

$$\frac{dq}{dt} = y(M - q(t)) + xw(t) - k(t)q(t), \tag{3}$$

$$\frac{dc}{dt} = k(t)q(t) - (l + r)c(t), \tag{4}$$

$$\frac{dw}{dt} = rc(t) - xw(t). \tag{5}$$

The model synapse output is a value proportional to the rate of transmitter release into the cleft, $k(t)q(t)$. The instantaneous release probability, $k(t)$, is the only stimulus-dependent variable in the model and is usually specified as a function of intracellular IHC voltage (defined as V_{IHC}, referenced to the IHC resting potential). Rapid adaptation after onset is the result of the depletion of the synaptic transmitters in the immediate store, and is mainly limited by the instantaneous release probability, $k(t)$. Short-term adaptation is the result of the depletion of synaptic materials available for recycling process, and is mainly limited by the reuptake rate [$rc(t)$], reprocessing rate [$xw(t)$], and the fraction of synaptic material in the cleft available for recycling, $r/(1+r)$. The replenishment of the synaptic transmitter from the global factory into the immediate store, $y[M-q(t)]$, contributes the model's steady-state response.

In the Westerman model, the transmitter reservoir is characterized by the volume, V, and concentration, C, of the synaptic material in the reservoir. The model (Fig. 2) has three reservoirs (global, local, and immediate) of synaptic material, connected in series by a diffusion path. The diffusion rate of synaptic material between reservoirs (from global to local, and then from local to immediate) is determined by the permeability (P) and by the concentration difference between the reservoirs. The governing equations for the transmitter release between these reservoirs are

$$V_I \frac{dC_I(t)}{dt} = -P_L C_I(t) - P_I(t) C_I(t) + P_L C_L(t), \tag{6}$$

and

$$\frac{dC_L(t)}{dt} = \frac{P_G C_G}{V_L} + \frac{P_L}{V_L} C_I(t) - \left(\frac{P_L + P_G}{V_L} \right) C_L(t), \tag{7}$$

where C_I, C_L, and C_G are the immediate, local, and global reservoir concentrations; V_I and V_L are the immediate and local reservoir volumes; and P_L and P_G are the permeabilities between the local and immediate and between global and local reservoirs, respectively.

The small immediate store (V_I, C_I) in the Westerman model is directly comparable with that in the Meddis model (q). The release permeability $P_I(t)$ is the same as $k(t)$ in the Meddis model, which is the only parameter determined by the input sound stimulus. The synapse output is a value proportional to the rate of transmitter released from the immediate store $[P_I(t)C_I(t)]$ into the synaptic cleft, similar to $k(t)q(t)$ in Meddis model. The Westerman model has the following characteristic function:

$$C_I(t) = \Phi_0' + \Phi_1' e^{-t/\tau_1'} + \Phi_2' e^{-t/\tau_2'}, \tag{8}$$

where the values of τ_1', τ_2', and Φ_0', Φ_1', Φ_2' can be calculated from Eqs. (6) and (7) (see Westerman and Smith, 1988). The primes in the parameter names distinguish these variables from those used in original Meddis model [see Eq. (13) below]. Note that the characteristic function here is the same as that of the onset responses of AN fibers [Eq. (1)].

Rapid adaptation in the Westerman model is the result of the depletion of the synaptic material in the immediate store and is mainly limited by the diffusion permeability of synaptic material from the immediate store to the cleft. Short-term adaptation is the result of the depletion of the synaptic material in the local store, and is mainly limited by the diffusion permeability between the local and immediate stores.

The local store (V_L, C_L) in the Westerman model is similar to the reprocessing store (w) in the Meddis model, which provides synaptic material for short-term adaptation. The synaptic material (w) in the Meddis model comes from very fast reuptake of released synaptic vesicles in the cleft, whereas the synaptic material in the Westerman model for rapid adaptation is stored in local store (V_L, C_L). The steady-state response in both models is attributed to the existence of the global store. In the Meddis model, the synaptic material from the global store is released directly into the immediate store (in parallel with the reprocessing store, w), whereas in the Westerman model, synaptic material enters the immediate store through the local store (which is cascaded with the immediate store).

III. MATHEMATICAL ANALYSIS OF THE MEDDIS AND WESTERMAN MODELS

The instantaneous release probability of a vesicle from the immediate store, $k(t)$, in the Meddis model [or $P_I(t)$ in the Westerman model] is usually a function of intracellular IHC voltage (V_{IHC}), which in turn is determined by the input sound stimulus. For a high-frequency tone burst, the IHC receptor potential V_{IHC} is dominated by the "dc" component (Russell and Sellick, 1978; Cheatham and Dallos, 1993), and it is reasonable to assume that $k(t)$ is a constant after the onset (denoted as k_2; the value of $k(t)$ before the onset is denoted as k_1). For further analysis, Eqs. (3)–(5) can be transformed into the Laplace (complex frequency) domain as follows, for $t > 0$:

$$sQ(s) - q(0^-) = yM/s - yQ(s) + xW(s) - k_2 Q(s), \tag{9}$$

$$sC(s) - c(0^-) = k_2 Q(s) - (l + r) C(s), \tag{10}$$

$$sW(s) - w(0^-) = rC(s) - xW(s), \tag{11}$$

where $q(0^-)$, $c(0^-)$, and $w(0^-)$ are the reservoir concentrations before the onset.

After solving for $Q(s)$,

$$Q(s) = \frac{(sq(0^-) + yM)(s + x)(s + l + r) + c(0^-)rxs + w(0^-)xs(s + l + r)}{s(s + x)(s + y + k_2)(s + l + r) - k_2 rxs}, \tag{12}$$

the characteristic function of $q(t)$ can be represented by

$$q(t) = \Phi_0 + \Phi_1 e^{-t/\tau_1} + \Phi_2 e^{-t/\tau_2} + \Phi_3 e^{-t/\tau_3}, \tag{13}$$

where $-1/\tau_i$ are poles of $Q(s)$. The values of τ_1, τ_2, τ_3, and Φ_0, Φ_1, Φ_2, Φ_3 can be calculated from $Q(s)$ directly.

Based on the parameters given in Meddis (1986, 1988) and Sumner *et al.* (2002), we can assume that l and $r \to \infty$ (or $l, r \gg x, y, k$), and we will let $u = r/(l+r)$. Thus, the following equations describe a simplified version of the Meddis model:

$$\frac{dq}{dt} = y(M - q(t)) - kq(t) + xw(t), \tag{14}$$

$$\frac{dw}{dt} = kuq(t) - xw(t), \tag{15}$$

$$C(s) = \frac{k_2 Q(s) + c(0^-)}{s + l + r}, \tag{16}$$

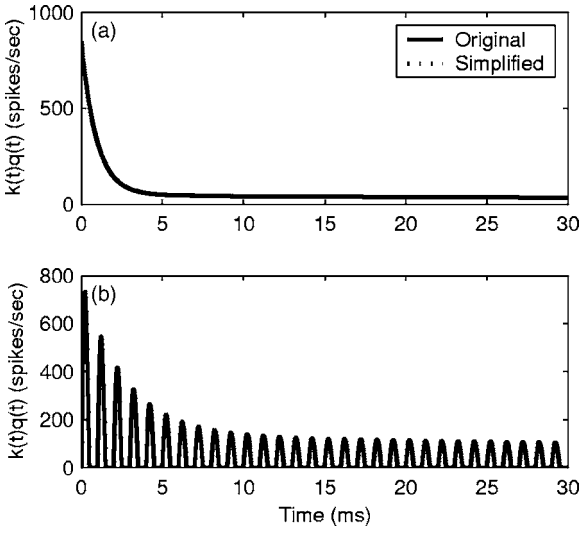

FIG. 3. Comparison of synapse output for the original Meddis model (solid line) and the simplified model (dotted line) described in the current study. Both models used the parameter values given in the Meddis study (1988): $l=2500$, $r=6580$, $x=66.31$, $M=1$, $y=5.05$. The responses from two models are essentially identical, as illustrated by the overlapping curves. (a) The analytical solution of $k(t)q(t)$ for both models for a constant stimulus, with $k_1=40.49$ and $k_2=1660$. (b) Simulation results of $k(t)q(t)$ for both models with a time-varying input $k(t)$ (a half-wave rectified sinusoidal wave form at 1 kHz with amplitude of k_2: $k(t)=0.5k_2[\sin(2000\ \pi t)+|\sin(2000\ \pi t)|]$).

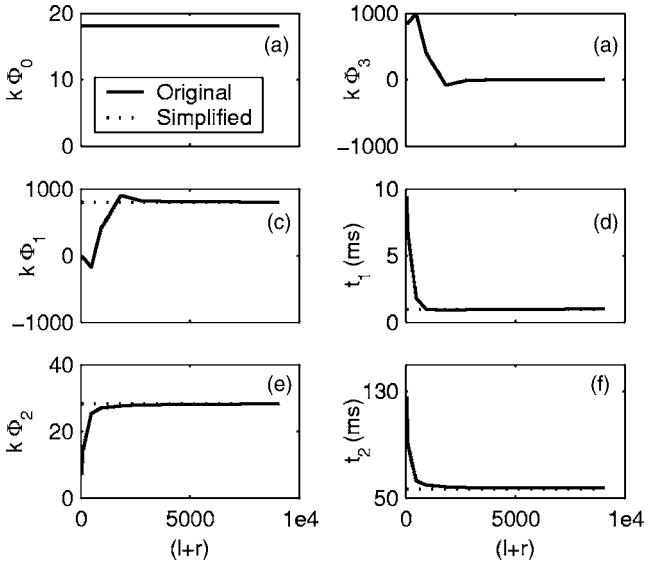

FIG. 4. The difference of each individual component (t_i and Φ_i) of $q(t)$ between the Meddis (1986) model and the simplified model as a function of $l+r$. The values of these components are constant for the simplified model (dotted line) because $u=r/(l+r)$ is kept the same for different values of $l+r$. The amplitude of the component (Φ_i) is scaled by k so it can be interpreted as the instantaneous firing rate of the synapse output. The values of corresponding components in the original model (solid line) all converge quickly to the values in the simplified model as $l+r$ increases, and the values are indistinguishable from each other when $l+r>5000$. The amplitude (Φ_3) of the additional component does not exist for the simplified model; in the original model, this amplitude converges to zero as $l+r$ increases and it can be neglected when $l+r$ is large.

$$Q(s)=\frac{(sq(0^-)+yM)(s+x)+w(0^-)xs}{s(s+x)(s+y+k_2)-k_2uxs}, \tag{17}$$

$$q(t)=\Phi_0'+\Phi_1'e^{-t/\tau_1'}+\Phi_2'e^{-t/\tau_2'}, \tag{18}$$

where again, the primes are meant to distinguish the parameters in the simplified model from those in the original model.

Figure 3(a) shows the comparison of the analytical solution of $k(t)q(t)$ for both the original model [Eq. (13)] and the simplified model [Eq. (18)] using the parameters given in Meddis (1988). Figure 3(b) compares simulation results from both models with the same input $k(t)$, a sinusoid wave form at 1 kHz. Both plots show that solutions from the simplified equations and the original equations are essentially identical, and the accuracy of the prediction does not depend on the input stimulus (e.g., whether it is stationary or nonstationary). These results also hold for other parameter sets given in other studies (Meddis, 1986, 1988; Sumner *et al.*, 2002; not shown). Thus, the simplified equations provide a good description of the Meddis model, and the solution [Eq. (18)] has two components with different time constants that are the same as those used to describe the characteristics of onset adaptation in AN fibers [Eq. (1)].

The accuracy of the simplified equations describing the Meddis model across different values of the sum $l+r$ is illustrated in Fig. 4. Each component of $q(t)$ (t_i and Φ_i) is plotted as a function of $l+r$ for both models (Fig. 4). The values of these components are constant for the simplified model because u is the same for different values of $l+r$. The values of corresponding components in the original model reach the values in the simplified model as the value of $l+r$ increases, and the values are indistinguishable from each other when $(l+r)>5000$ (the values of $l+r$ used in the Meddis (1986, 1988) were usually greater than 15 000). The amplitude (Φ_3) of the additional component in the original model can be neglected compared to the other components when the value of $l+r$ is large. A detailed interpretation of the relationship between the simplified and original Meddis models is further explained in Sec. VI.

Because $k(t)$ and $P_I(t)$ are the only stimulus-dependent variables in the simplified Meddis and Westerman models, the two models can be compared more directly by substituting $k(t)$ with $P_I^M(t)$ and $q(t)$ with $C_I^M(t)$ in Eqs. (14) and (15). The constant yM in Eq. (14) can be removed by substituting $w(t)$ with $[(y+xu)/x][C_L^M(t)-yM/x-uC_I^M(t)]$. After making these changes, we have the following equations describing the simplified Meddis model:

$$\frac{dC_I^M}{dt}=-(y+xu)C_I^M(t)-P_I^M(t)C_I^M(t)+(y+xu)C_L^M(t), \tag{19}$$

$$\frac{dC_L^M}{dt}=\frac{xyM}{y+xu}+xu\left(\frac{x}{y+xu}-1\right)C_I^M(t)-x(1-u)C_L^M(t). \tag{20}$$

Since there is one free parameter in Westerman's model, we can always assume $V_I=1$ (that is, we can decrease V_I, V_L, P_I, P_L, P_G and increase C_I, C_L, C_G by the same scale, V_I, and the synapse output P_IC_I remains the same). It is obvious that the equations describing the two models [Eqs. (6), (7), (19), and (20)] are directly comparable. If we set the correspond-

ing parameters to the same values (e.g., $P_L = y + xu$), then the synaptic response of the simplified Meddis model $[k(t)q(t)]$ and that of the Westerman model $[P_I(t)C_I(t)]$ to arbitrary inputs should be exactly the same.

IV. DERIVING MODEL PARAMETER VALUES FROM PERI-STIMULUS TIME HISTOGRAM PROPERTIES: THE RELATIONSHIP BETWEEN MODEL PARAMETERS AND ADAPTATION CHARACTERISTICS

The values of the parameters in the onset adaptation function [Eq. (1)] are usually determined by fitting this characteristic equation to the PST histogram of AN fiber responses. The refractoriness in the PST histograms can be removed before fitting (Westerman and Smith, 1988), so the IHC-AN synapse output (instantaneous firing rate) can be more accurately represented by the characteristic function.

With these adaptation parameters $(A_{\text{sus}}, A_r, A_{\text{st}}, \tau_R, \tau_{\text{ST}})$ and the spontaneous rate (A_{sp}) of the AN fibers, the values of parameters in both models can be derived. The analytical solution for the Westerman model is reported in previous studies (Westerman and Smith, 1988; Zhang *et al.*, 2001). The derivation of the analytical solution for the values of the parameters in the simplified Meddis model from these characteristic parameters is given in the Appendix. Since any desired adaptation responses can be obtained from both models with appropriate parameters, comparing adaptation responses for different models with specific parameters will not give us any insight concerning these models.

It is important to note that the mapping from V_{IHC} to $k(t)$ in the Meddis model, or $P_I(t)$ in the Westerman model, should change with the fiber adaptation characteristics: each adaptation characteristic requires different sets of the model parameters (including the permeability at rest and the permeability at any other desired level); the spontaneous rate, rate threshold, and rate-level function curve differ among fiber types that require different V_{IHC}-k (V_{IHC}-P_I) relationships. An appropriate V_{IHC}-k (V_{IHC}-P_I) representation is critical for a composite model that successfully describes AN responses (Heinz *et al.*, 2001; Sumner *et al.*, 2002). The procedure for deriving the appropriate V_{IHC}-k (V_{IHC}-P_I) function combining the results in the present study and recent developments of these models are further discussed in Sec. VI.

Though the same desired adaptation responses can be obtained from both models, the dependence of the parameters in each model upon various adaptation characteristics differs. Also, because the models have different structures, these parameters have specific physical meanings in each model. A survey of how these parameters change with different model-AN fiber types will provide valuable information and further our understanding of both models.

Figures 5 and 6 show an example of how the parameters change systematically for different model-AN fiber types in the simplified Meddis model and Westerman models, respectively. Other possible ways to specify the adaptation across different model-AN fiber types are detailed in Sec. VI. Here, the fiber types are described by the peak-to-sustained ratio $[\text{PTS} = (A_r + A_{\text{st}} + A_{\text{sus}})/A_{\text{sus}}]$ of the onset adaptation, which changes with spontaneous rate, A_{sp} (Rhode and Smith, 1985), as described by the following equation:

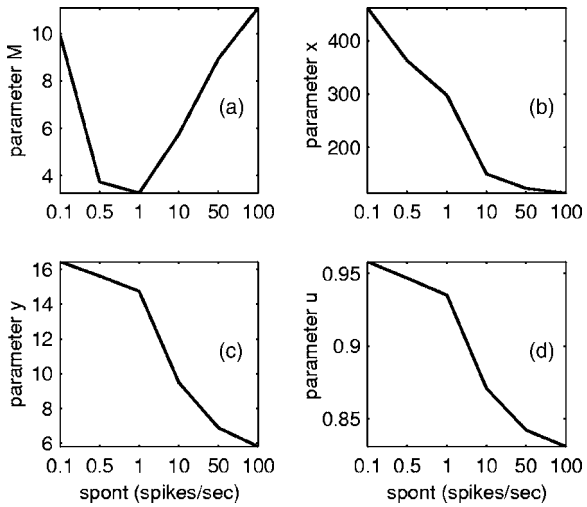

FIG. 5. The relationship between parameter values (M, x, y, and u) and spontaneous rate for the Meddis model. Other adaptation parameters used to derive the model parameters are: $\text{PTS} = (A_r + A_{\text{st}} + A_{\text{sus}})/A_{\text{sus}} = 1 + 9A_{\text{sp}}/(9 + A_{\text{sp}})$, $\tau_R = 2$ ms, $\tau_{\text{ST}} = 60$ ms, $A_r/A_{\text{st}} = 6$, and $A_{\text{sus}} = 350$. The value of M in the Meddis model changes nonmonotonically with increasing spontaneous rate; all other parameters decrease as spontaneous rate increases.

$$\text{PTS} = 1 + 9 \times A_{\text{sp}}/(9 + A_{\text{sp}}). \tag{21}$$

The other adaptation parameters are held constant across model AN fibers ($\tau_R = 2$ ms, $\tau_{\text{ST}} = 60$ ms, $A_r/A_{\text{st}} = 6$, $A_{\text{sus}} = 350$). The parameter values from Fig. 5 for several specified spontaneous rates are given in Table I. Figure 5(a) shows that the value of M in the Meddis model changes nonmonotonically with increasing spontaneous rate; it drops initially and then increases from 3 to 10 as spontaneous rates increase from 1 to 100 spikes/s. All other parameters (x, y, and u) in the Meddis model decrease continuously as the model's spontaneous rate increases. The parameter changes in Westerman's model are plotted in Fig. 6. The global concentration (C_G) was always set to 1

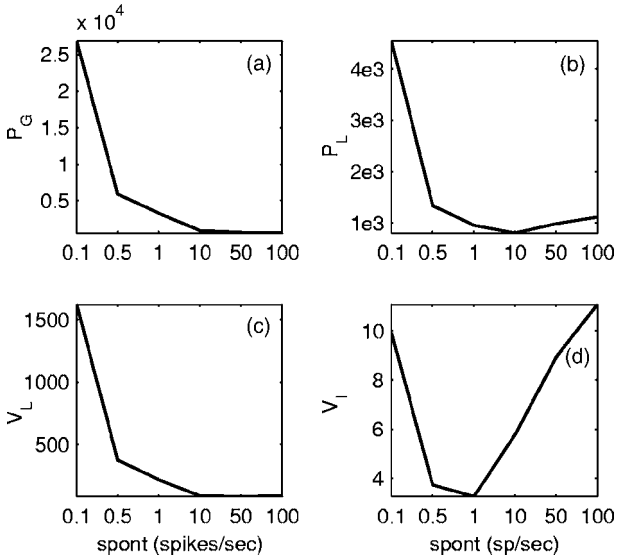

FIG. 6. The relationship between parameters (P_L, P_G, V_L, V_I) and the spontaneous rate in the Westerman model. The other adaptation parameters are the same as in Fig. 5. The parameters were derived with global concentration (C_G) equal to 1.

TABLE I. Parameters in the simplified Meddis model for several fiber types, specified by the spontaneous rate in parentheses in the first column.

	x	y	M	u	$k1$	$k2$
HSR (60)	120.3	6.63	9.4	0.84	7.6	389.7
MSR (10)	149.6	9.48	5.8	0.87	1.78	357.6
LSR (0.1)	461.4	16.43	9.9	0.96	0.01	38.80

before determining the other parameter values. The trends in the value of the immediate volume, V_I [Fig. 6(d)], are similar to those of M observed in Fig. 5(a). Other parameters (P_G, P_L, and V_L) decrease initially and then are insensitive to the value of spontaneous rate above 5 spikes/s.

The A_{sus} defined in the adaptation parameters is the sustained rate at a certain stimulus level. The level is not specified here but is presumably a high level determined by the level-permeability function in the rest of the composite model for the AN response. The values of model parameters derived from these adaptation parameters are specified for this level (a medium or high level for high-spontaneous-rate model fibers, and a very high level for low-spontaneous-rate model fibers). The assumption of both models is that all of these parameters except one (P_I in Westerman model, and k in Meddis model) are constant across different levels. The adaptation characteristics of the models change as the value of the level-dependent parameter changes. When the level-dependent permeability (P_I, or k) increases, the sustained rate in both models saturates at a value:

$$A_{\text{sus\_MAX}} = \lim_{Pi\to\infty} P_I C_I = \frac{P_L P_G C_G}{P_L + P_G} = \lim_{k\to\infty} kq = \frac{yM}{1-u}. \quad (22)$$

The value of $A_{\text{sus,\_MAX}}$ also changes with the AN fiber's spontaneous rate (see Fig. 7): The value for high-spontaneous-rate model fibers is comparable to A_{sus}, whereas $A_{\text{sus\_MAX}}$ increases rapidly as spontaneous rate decreases. The results above may suggest a fundamental difference between low- and high-spontaneous-rate AN fibers: The high-spontaneous rate fibers have a saturated response rate around A_{sus} with an input level higher than specified, and low-spontaneous-rate fibers will not have a saturated response at higher levels due to a much larger $A_{\text{sus\_MAX}}$ value than that of A_{sus}.

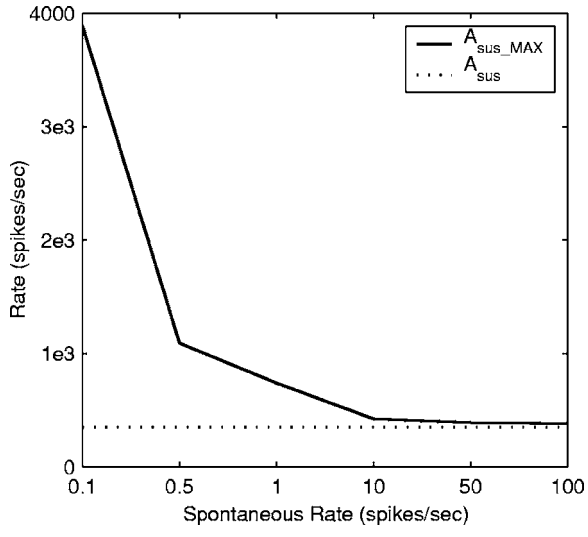

FIG. 7. The maximum sustained rate [$A_{\text{sus\_MAX}}$, solid line; see Eq. (22)] for both Meddis and Westerman models as a function of model spontaneous rate. The other adaptation parameters are set as in Fig. 5 (thus, A_{sus} has a constant value, as shown by the dotted line). The value of $A_{\text{sus\_MAX}}$ for high-spontaneous rate model fibers is comparable to A_{sus}, whereas the value increases rapidly as spontaneous rate decreases.

It is also possible to study analytically the effects of the model parameters on adaptation characteristics with the solution given above. For example, Eq. (17) is the analytical solution for the simplified Meddis model. The steady-state value of q is given by:

$$q_\infty = sQ(s)|_{s=0} = \frac{yM}{y + k_2(1-u)}. \quad (23)$$

If we denote k_L as the value of k at a specified sound stimulus level (L), the steady-state response rate, $R(L)$, can be derived:

$$R(L) = k_L q_\infty = \frac{k_L yM}{y + k_L(1-u)}. \quad (24)$$

With the values of the other model parameters fixed, the model's steady-state response $R(L)$ changes proportionally with the value of M. Sumner *et al.* [2002, Fig. 5(c)] reported the simulation results of rate-level functions with different values of M. Their results and comments are in fact a direct reflection of the relationship explained in Eq. (24).

Since P_I (or k in the Meddis model) is level dependent, changes of the model adaptation response as a function of the value of P_I after onset represent the effect of level on the model onset characteristics. If we set the value of P_I before onset (P_{I1}) to another value, we can also study the model adaptation responses to increments and decrements using the same paradigm (a comprehensive survey of adaptation in the Meddis model with specified parameters is provided by Sumner *et al.*, 2003).

Figure 8 shows the change of components of the model onset adaptation as a function of the value of immediate permeability P_I after onset (or k in the Meddis model) for a model IHC-AN synapse with spontaneous rate of 50 spikes/s. The model has a spontaneous response with permeability of P_{I1} when there is no stimulus input. The sustained rate (A_{sus}) is roughly saturated at permeability P_{I2}, which generates the desired onset adaptation, while the contribution of short-term and rapid components continues to change as the permeability P_I increases [Fig. 8(a)]. Both the rapid decay time constant and short-term decay time constant decrease as P_I increases [Fig. 8(b); note that τ_R is multiplied by 10 in this plot]. For the simplified Meddis model, these two time constants are determined by the poles in Eq. (17), and values of $-1/\tau_R$ and $-1/\tau_{\text{ST}}$ are the roots of the polynomial function in the denominator. The values of τ_R and τ_{ST} can be approximated by $1/k$ and $1/(x-ux)$ when $k \gg x, y$ (i.e., at a medium or high stimulus level for this model fiber). For the model illustrated in Fig. 8, the short-term time constant is about 120 ms at rest and decreases to 50 ms at high levels, and the rapid time constant is 8 ms at rest and de-

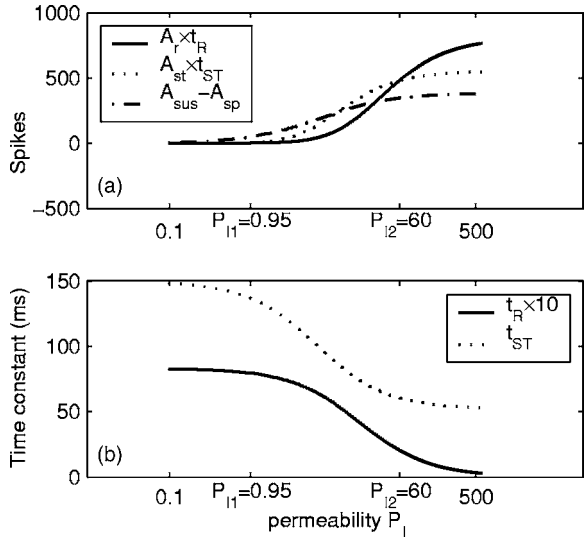

FIG. 8. Effects of the model parameter, P_I, (for the Westerman model) on onset adaptation characteristics. The model parameters were derived from adaptation properties specified in Fig. 5 with a spontaneous rate of 50 spikes/s. The values of P_{I1} and P_{I2} are the values of the immediate permeability before and after the stimulus onset. (a) The contribution of each PST onset component. The contribution of the rapid component (solid line) and short-term component (dotted line) are the integrals of their exponential functions (and thus have units of spikes). The contribution of the constant component (sustained rate–spontaneous rate; dashed line) saturates as P_I increases. (b) Both rapid and short-term time constants decrease as the permeability increases. The rapid time constant (τ_R, solid line) is multiplied by 10 to allow it to be plotted with the short-term time constant (τ_{ST}, dotted line).

creases continuously as the input sound level increases (the value we chose to derive the model parameters was τ_{ST} =60 ms, τ_R=2 ms). Since onset adaptation cannot be estimated accurately at low sound levels from physiological responses, these time constants in the model at rest are more related to other adaptation characteristics (e.g., offset adaptation, as discussed in next section, or recovery of onset adaptation).

V. MODIFYING THE SYNAPSE MODEL TO OBTAIN THE DESIRED OFFSET ADAPTATION RESPONSE

The above analysis shows that the model parameters can be determined on the basis of onset adaptation characteristics (at a certain stimulus level). When the model parameters are set, the other adaptation characteristics of the model synapse are automatically determined. If we set the level-dependent permeabilities P_{I1} and P_{I2} (k_1 and k_2 in the Meddis model) to the values before and after the stimulus offset, the analytical solution from Eq. (8) also provides a description of the responses of the model synapse after stimulus offset.

A direct conclusion is that the offset adaptation of the model synapse is also a sum of two exponential functions. The time constants of these two components are determined by P_I after offset and limited by the time constant at the onset. Since only P_{I2} affects the time constant [see Westerman and Smith, 1988, for Westerman's model and Eq. (17) for the Meddis model], Fig. 8(b) also shows how the time constant in the offset adaptation changes with the permeability after offset. Physiological studies (Smith and Zwislocki, 1975; Smith, 1977; Westerman, 1985) suggest that AN fibers with medium- or high-spontaneous rate usually stop responding immediately after offset (which begins the deadtime period) and recover slowly with a time constant longer than that of short-term adaptation. However, the rapid component of the model recovery function causes the synapse to recover quickly after stimulus offset. Since $P_I(t)$ and $C_I(t)$ cannot be negative, the magnitude of these recovery components [ϕ_1', ϕ_2' in Eqs. (8) and (18); the sign of these components is negative at stimulus offset] is also limited by the value of ϕ_0' (determined by the spontaneous rate). Because of these limitations, the offset adaptation of the model response is unrealistic as compared to the physiological responses specified in Eq. (2).

The function fitting offset adaptation responses has another general form (Harris and Dallos, 1979):

$$R_{\text{off}}(t) = (A_{\text{sp}} - A_{\text{min}})(1 - e^{-t/\tau_{\text{sp}}}) + A_{\text{min}} \quad \text{for } R(t) > 0$$
$$= 0 \quad \text{for } R(t) < 0, \tag{25}$$

where A_{min} is a negative value that accounts for the deadtime period of the offset response. Since an AN fiber has a very low probability of response during the deadtime period, the recovery process is not well studied, and there may be a rapid recovery component that corresponds to the onset rapid adaptation and becomes insignificant before the end of the deadtime period. The offset characteristic function can thus be described as:

$$R_{\text{off}}(t) = (A_{\text{sp}} - A_{\text{min}})(1 - e^{-t/\tau_{\text{sp}}}) + A_{\text{min}} + A_r^{\text{off}} e^{-t/\tau_r^{\text{off}}} \quad \text{for } R_{\text{off}}(t) > 0$$
$$= 0 \quad \text{for } R_{\text{off}}(t) < 0, \tag{26}$$

where A_r^{off} is the magnitude (with a negative value) and τ_r^{off} is the time constant of rapid recovery component. Since the model synapse output $P_I C_I$ in the Westerman model cannot be negative, we can assume that the measured synapse output is:

$$R_{\text{off}}(t) = P_I(t) C_I(t) - A_{\text{shift}} \quad \text{for } R_{\text{off}}(t) > 0$$
$$= 0 \quad \text{for } R_{\text{off}}(t) < 0, \tag{27}$$

where A_{shift} is a shift value to guarantee that $P_I C_I > 0$, for all t, and that $R_{\text{off}}(t)$ is the same offset adaptation function as in Eq. (26) (thus $A_{\text{shift}} > |A_r^{\text{off}}| + |A_{\text{min}}|$). The onset of the model synapse output now becomes

$$P_I(t) C_I(t) = R_{\text{on}}(t) + A_{\text{shift}}$$
$$= A_{\text{shift}} + A_{\text{sus}} + A_r e^{-t/\tau_r} + A_{\text{st}} e^{-t/\tau_{\text{st}}}. \tag{28}$$

Thus, by including this shift, the same equations can describe adaptation of both the onset and offset in the Westerman model. By substituting $P_I(t)C_I(t)$ with $k(t)q(t)$ in Eqs. (27) and (28), the same procedure can be applied to the Meddis model to obtain the desired onset and improved offset adaptation using the same equations.

Figure 9 shows the onset and offset responses of the synapse model with or without the shift. The value of the model parameters was derived to have the same onset adap-

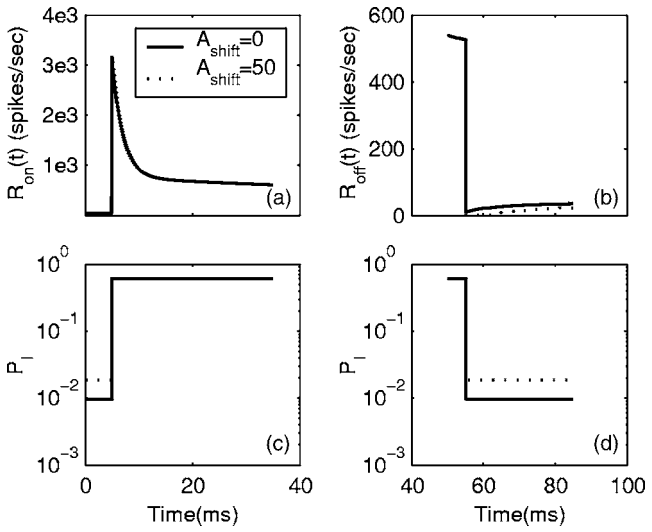

FIG. 9. Onset and offset responses of the Westerman model with (dotted line) or without (solid line) the shift value added. The shift value is set to 50 spikes/s. (a) The model onset responses are unchanged because the model parameters were derived to have the same onset adaptation. (b) The model offset response with the shift recovers more slowly than does the model offset response without the shift and has the desired deadtime period. (c), (d) The permeability $P_I(t)$ jumps from P_{I1} to P_{I2} at the onset (5 ms) and drops back to P_{I1} at the offset (55 ms). The model parameters (e.g., P_{I1}) were changed to maintain the same onset response.

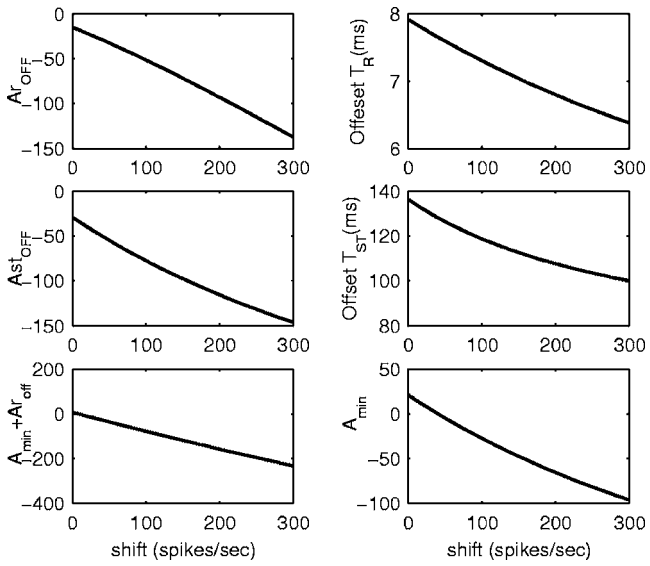

FIG. 10. Effects of the parameter A_{shift} in Eq. (27) on the model offset components. The model parameters are derived so they have the same onset adaptation with different A_{shift} values [spontaneous rate A_{sp}=50, A_{sus}=350, PTS=$(A_r+A_{st}+A_{sus})/A_{sus}$=9, τ_R=2 ms, τ_{ST}=60 ms, A_r/A_{st}=6.0; see Eq. (1)]. The upper plots illustrate how the magnitude and time constant of the offset rapid component changes as a function of shift; the middle plots show changes of the offset short-term component. The time constants for both components decrease as shift increases and are larger than the corresponding onset time constants. The rapid component recovers quickly (usually during the deadtime period) and the recovery time constant is thus determined by the short-term component. The magnitude of this component is always negative and decreases (becomes more negative) as the shift increases. A_{min} [bottom right; see Eqs. (25) and (26)] changes from positive to the desired negative as the shift value increases; A_{min} and the time constant of the short-term component determine the duration of the deadtime period. The plot at the bottom left shows the most negative value (including the contribution of the rapid component, which recovers quickly) of the model response without rectification [$R_{off}(t=0)$ in Eq. (24)] as a function of the shift value.

tation. The permeability $P_I(t)$ jumps from P_{I1} to P_{I2} at 5 ms and drops back to P_{I1} at 55 ms. When the shift (A_{shift}=50) was added, the model parameters [e.g., P_{I1} in Figs. 9(c) and 9(d)] were changed to maintain the same onset response. Thus, the original model and modified model have the same onset responses [Fig. 9(a)] while the modified model has a greatly improved offset adaptation response [Fig. 9(b)].

The effect of A_{shift} on the offset components is illustrated in Fig. 10. Since the rapid component recovers quickly during the deadtime period, the offset adaptation process is dominated by the short-term component. The magnitude of the short-term component [$A_{min}-A_{sp}$ in Eq. (25)] determines the duration of the deadtime period, and the time constant (τ_{ST}) determines the value of the recovery time constant τ_{SP}. The recovery time constant is always greater than that of the onset short-term adaptation (60 ms), although the value decreases as the shift is increased. The value of A_{min} [Eq. (25)] becomes more negative with a larger shift, which produces the desired deadtime period.

The offset adaptation properties of the IHC-AN synapse could account for enhanced phase locking to the stimulus envelope in AN fibers. The AN fibers were less responsive during the dip of the envelope because of the offset adaptation, and thus the fibers were more synchronized to the peak of the envelope. Figure 11 illustrates the effects of offset adaptation on the modulation transfer function [(MTF), see Joris and Yin, 1992, for a comprehensive experimental study] for a model AN fiber (Zhang *et al.*, 2001) to a sinusoidally amplitude-modulated stimulus.[1] The IHC-AN synapse component of that model was replaced with the synapse model presented here (the onset adaptation parameters were the same as in previous study), and a different shift value was used to represent offset adaptation (i.e., a shift value of 0 means the synapse model was the same as the original model). The stimulus was always fully modulated (modulation index m=1) at 10 dB sound pressure level (SPL), with the carrier frequency set equal to the AN CF of 21 kHz. The model AN fibers with offset adaptation (e.g., with a larger shift value) had increased modulation gain and an enhanced MTF that was more consistent with the data from physiological experiments (Joris and Yin, 1992).

VI. DISCUSSION

In this section, we first discuss the differences and similarities between the different models under investigation. We then discuss how to use the analytical methods developed in the present study to further our understanding of adaptation in models and in the IHC-AN synapse. We consider different adaptation measures that can be used to describe a single AN fiber, as well as the fact that different adaptation properties may be observed for different AN fiber types. Finally, we discuss how to extend the analytical method to other models and identify the candidate model that represents the actual underlying physiological mechanism.

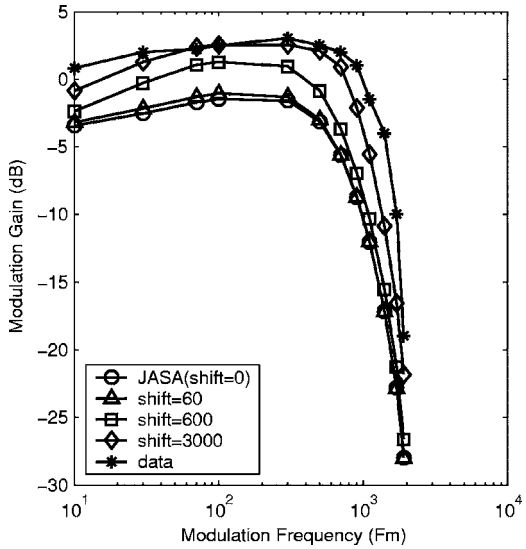

FIG. 11. Modulation transfer function for the model AN fibers. The stimulus was always fully modulated at 10 dB SPL with carrier frequency at AN CF of 21 kHz, gated with a 10-ms cosine-square function. The modulation gain was defined as $20\log[(\text{modulation of responses})/(\text{modulation of stimulus})]$ (i.e., modulation gain$20\log(2R/m)$, where R was the vector strength of the AN responses and m was the modulation depth; see Joris and Yin, 1992). The model AN fibers with larger shifts in the synapse had higher modulation gain and were more consistent with the data from physiological experiments (asterisks in the figure, from Joris and Yin, 1992).

A. Interpretation and justification of the simplified Meddis model

The loss rate, l, in the cleft of the original Meddis model, was represented in the simplified model by the fraction of synaptic material recycled, $u=r/(l+r)$, where r is the reuptake rate. The difference between the simplified and original model centers on the following questions: Is the recycling of synaptic material in the cleft a two-stage process, as in the original Meddis model, or a one-stage process, as in the simplified model (by assuming reuptake rate r is much larger than w and removing it)? Or, to put the question another way, is the phenomenological one-stage process of the simplified model sufficient to describe the recycling mechanism instead of the two-stage process in the original Meddis model?

With a value of r much larger than the values of x and k, the one-stage process in the simplified model definitely generates the same response as that of the two-stage process in the original Meddis model (see Fig. 4). Even when the value of r decreases to a value comparable to k (still much larger than x), the responses from the simplified model are still almost the same as those of the original model, since the recycling process contributes to the short-term adaptation, which is mainly determined by the value of x. For values of $l+r$ between 1000 and 5000 (Fig. 4), the amplitude and time constant of short-term adaptation does not change much, and the additional component (ϕ_3) which contributes to the rapid adaptation increases at the expense of another rapid component, ϕ_1. For a very small value of r, both reuptake (r) and reprocessing (x) will affect the short-term adaptation in a complex way for the original Meddis model.

It then becomes a question of whether the model with small values of r and x could predict the adaptation of the IHC-AN synapse. It is not surprising that the exercise of finding model parameters to provide a satisfactory description of adaptation responses ended up with the large value of r in the original Meddis model (Meddis, 1986, 1988; Sumner *et al.*, 2002). These findings justify our simplification of the original Meddis model.

When the value of k becomes extremely high (infinite) after the onset in the original Meddis model, all of the transmitter, $q(0^-)$, in the immediate pool is released into the cleft instantaneously right after the onset. The amount of transmitter in the cleft increases instantly and becomes $q(0^-)+c(0^-)$. Thereafter, all transmitter replenished from the reprocessing store (w) and the global factory into the immediate pool is released into the cleft instantaneously:

$$kq = y\mathrm{M} + xw. \tag{29}$$

The dynamics of the original Meddis model are now governed by Eqs. (4), (5), and (29). The solution of these equations in the Laplace domain is given by:

$$C(s) = \frac{(yM + c(0^-) + q(0^-))(s+x) + xw(0^-)s}{s(s+r/u)(s+x) - rxs}, \tag{30}$$

where u is defined as the fraction of transmitters recycled, $u=r/(l+r)$.

If the synapse output is proportional to the amount of transmitter in the cleft $c(t)$, the responses in the original Meddis model can again be characterized by Eq. (18), based on Eq. (30). The steady-state response in the original Meddis model is also specified by Eq. (24), and is independent of the value of r. The rapid adaptation time constant (τ_R) can be approximated by u/r, or $1/(l+r)$, when $r/u \gg x$, and this value of τ_R is independent of k at high stimulus levels (k is very large). Thus, with an appropriate value of $l+r$, the original Meddis model is a better candidate than the simplified Meddis model in predicting the changes of the adaptation time constants at high stimulus levels (Westerman, 1985). In reality, the composite AN model with the original Meddis synapse model usually has k operating within a limited range, and thus the original Meddis model can be perfectly replaced by the simplified Meddis model.

B. Physiological assumptions underlying the Westerman and Meddis models

This study shows that two phenomenological IHC-AN synapse models that were designed to explain the onset adaptation characteristics of AN responses are essentially the same. It is impossible to differentiate these two models by evaluating their adaptation responses. There are many similarities between the Westerman and Meddis models. Rapid adaptation is modeled as a depletion of the synaptic material in the immediate store in both models, which is supported by recent physiological studies (Moser and Beutner, 2000).

The sustained response of the IHC-AN synapse in both models is attributed to the replenishment of synaptic material from the global store to the immediate store, either directly or indirectly. For model fibers with little adaptation but considerable sustained response rate (e.g., some low-

TABLE II. Adaptation characteristics derived from three model fibers specified in Sumner *et al.* (2002). The values of M, spontaneous rate, and sustained rate of fibers are specified in the first three columns. The sustained response rate of fibers is always 10 spikes less than the maximum response described in Eq. (22). The values of other model parameters are from Sumner *et al.* (2002): $y=10$, $x=66.3$, $l=2580$, $r=6580$. The values of $k1$ and $k2$ are then derived from Eq. (24), and the other adaptation characteristics are derived from the simplified Meddis model.

	M	A_{sp}	A_{sus}	$k1$	$k2$	τ_R (ms)	A_r (spikes/s)	τ_{ST}(ms)	A_{st} (spikes/s)
H1	10	60	345	7.2202	1225	0.78	9660	54.5	174.6
M1	13	10	451	0.7863	1603	0.60	19667	54.3	271.6
L1	8	0.1	274	0.0125	972.9	0.97	7340	54.7	167.0

spontaneous-rate fibers), the replenishment rate of synaptic material from the global pool into the immediate store must be comparable to the release rate of synaptic material from the immediate store into the cleft. For the Meddis model, either a small k or large y at high levels is needed for these model fibers (or both; see Table I and Fig. 5). To overcome this limitation, another global store that releases synaptic materials directly into the cleft can be included to generate the sustained response. This parallel global synaptic store separates the sustained response from adaptation, and adaptation across different fibers can be adjusted by changing the value of M (or C_G in the Westerman model) instead of the value of the replenishment rate of synaptic material into the immediate store.

The key difference between two models is that short-term adaptation is accounted for by the recycling of the synaptic material from the cleft in the Meddis model and by depletion in the Westerman model. Recent physiological studies (Moser and Beutner, 2000) show that the time constant of endocytosis is about 7.5 s in the IHC-AN synapse. However, in the Meddis model, the recycling rate of synaptic material in the cleft must be set to a time scale of approximately 10 ms to account for short-term adaptation. Thus, the model time constant is about 100 times faster than the value obtained in physiological studies.

In the Westerman model, it is assumed that short-term adaptation does not come from endocytosis, and the recycling process is not included in this model. Instead, short-term adaptation is modeled as the depletion of synaptic materials in the local store. Of course, it is entirely possible that the physiological assumptions in both models are wrong, but that the models work because they are sufficient models for representing actual physiological mechanisms that are unknown.

C. Different adaptation measures for single auditory-nerve fibers

Other than onset and offset adaptation, there are many other measures of adaptation: Recovery after offset (Harris and Dallos, 1979; Westerman, 1985), responses to increments (Smith and Zwilocki, 1975; Smith *et al.*, 1985), decrements (Smith *et al.*, 1985), and conservation (Westerman, 1985). Sumner *et al.* (2003) provided a comprehensive survey of these adaptation measures in a recently developed version of the Meddis model, with several sets of model parameters specified. These results can be applied to the Westerman model quite naturally since the two models are essentially the same, with the appropriate parameters specified. Our analytical results allow the adaptation characteristics to be derived directly from the specified model parameters (Table II).

Instead of evaluating whether specified model AN fibers can predict different measures of adaptation, our analytical results can provide insights for the limitations of these models, and explain the performance of these models for different adaptation measures. For example, Fig. 8 showed the changes of onset adaptation components with the stimulus-level-dependent variable k in the simplified Meddis model (or P_I in the Westerman model). The rapid and short-term adaptation time constants, τ_R and τ_{ST}, approach $1/k$ and $1/(x-ux)$, respectively, as the value of k increases. The value of τ_R is more affected by the value of k than that of τ_{ST}, especially when they are plotted on a log scale. These results explain the simulation results reported by Sumner *et al.* (2003), and provide insights into the failure of these models in predicting the changes of the rapid adaptation time constant at low sound levels.

For the Westerman model, recovery after stimulus offset of the onset rapid and short-term adaptation can be interpreted as the replenishment of the synaptic material in the immediate and local stores. The recovery time constant of rapid adaptation is thus determined by the permeability, P_L, between the local and immediate stores, which also determines the time constant of short-term adaptation (depletion of synaptic material in the local store) at onset. This explains why the recovery time constant of rapid adaptation is comparable to the short-term adaptation time constant instead of that of rapid adaptation, consistent with both physiological studies (Westerman, 1985; Moser and Beutner, 2000) and simulation studies (Sumner *et al.*, 2003).

The analytical results from these models show that different adaptation measures are highly correlated for a single model IHC-AN synapse. It is of great interest to see how these adaptation measures are correlated in the physiological responses of single AN fibers. The correlation studies of adaptation measures across AN fibers may be limited by the variation of physiological properties across AN fibers.

The values of model parameters can be derived from adaptation characteristics at different stimulus levels (Westerman and Smith, 1988). When more than one model parameter varies with level, the underlying assumptions of the method used here to generate the model parameters (e.g., allowing only P_I or k to change with level) is invalidated. In this situation, it is more mathematically challenging to estab-

lish the relationship between adaptation characteristics and model parameters. On the other hand, when this level-dependent relationship is established using more complex techniques, the model may provide more accurate predictions for different measures of IHC-AN adaptation, and it may also provide insights into the physiological properties specified by the model parameters.

D. Adaptation across different auditory-nerve fiber types and transmitter release functions in model auditory-nerve fibers

Our analytical approach makes it possible to link adaptation characteristics directly to the values of model parameters. Making models to predict adaptation across AN fiber types then becomes a question of how to determine different adaptation characteristics across AN fiber types. In the present study, we considered the example of a description of different fiber types based on the peak-to-sustained ratio [$\mathrm{PTS}=(A_r+A_{\mathrm{st}}+A_{\mathrm{sus}})/A_{\mathrm{sus}}$] of the onset adaptation, which changes as a function of spontaneous rate, A_{sp} (Rhode and Smith, 1985) [Eq. (21)]; other parameters were fixed across different fiber types ($\tau_R=2$ ms, $\tau_{\mathrm{ST}}=60$ ms, $A_r/A_{\mathrm{st}}=6$, $A_{\mathrm{sus}}=350$). For low-spontaneous-rate fibers with PTS close to a value of 1, values of A_r and A_{st} are very small. Since there is little contribution of these adaptation components to AN fiber responses, the values of other parameters (τ_R, τ_{ST}, and A_r/A_{st}) may not be determined with confidence based on a fit of the PST histograms, and models with a wide range of parameter values can provide equally good fits to the AN fiber responses.

It is possible to determine adaptation characteristics using the results of other experimental paradigms. Relkin and Doucet (1991) found that the recovery time constant for low-spontaneous-rate fibers is much larger than that of high-spontaneous-rate fibers, and the small peak-to-sustained ratio observed for low-spontaneous-rate fibers (Rhode and Smith, 1985) may have been partly determined by the short interstimulus intervals used to study them (105 ms for Rhode and Smith, 1985). The relationship between adaptation characteristics of different measures and model parameters can be created using our analytical approach, and values of model parameters can be derived accordingly.

When some characteristics of adaptation cannot be determined with confidence by fitting the PST histograms for certain AN fiber types (e.g., low-spontaneous-rate fiber), it is reasonable to fix some model parameters across all model fiber types (e.g., y for the Meddis model, or P_G for the Westerman model), and then derive the values of the other parameters in the model. The assumption underlying this method is that the corresponding physiological property specified by the model parameter does not change across different fiber types. It would be very interesting to see how these corresponding physiological properties varied across the IHC-AN synapse in physiological studies.

In addition to specifying the model parameters to explain adaptation, it is also critical to find an appropriate transmitter release function for the AN model fiber to generate desired rate-level responses. The relationship between IHC voltage (V_{IHC}, referenced to the IHC resting potential), which is stimulus dependent, and release rate from the immediate store (k in the Meddis model, or P_I in the Westerman model) is highly simplified and usually specified by an *ad hoc* function in most modeling studies.

For the Meddis model, the relationship between the steady-state response rate and k is specified in Eq. (24), and the rate-level function is further determined by the V_{IHC}-k relationship. For a simple linear V_{IHC}-k relationship, the value of k at rest ($V_{\mathrm{IHC}}=0$) determines the spontaneous response of the model fiber, and the slope of the V_{IHC}-k function determines how fast the response will approach saturation [$A_{\mathrm{sus\_MAX}}$ in Eq. (22)] and whether or not the rate-level function will saturate. It is thus not surprising that equivalent parameters in these models varied across different model fiber types (Heinz *et al.*, 2001; Sumner *et al.*, 2002), and that the values of these parameters affected the shape of the rate-level functions in simulations [Figs. 5(a) and 5(b) in Sumner *et al.*, 2002, Fig. 1 in Sumner *et al.*, 2003].

Another useful conclusion from Eq. (22) is that the saturation of the synapse response is largely contributed by the synapse model itself, rather than by saturation of the value of k (or P_I). The fact that P_I does not saturate as V_{IHC} increases at high levels (Carney, 1993; Zhang *et al.*, 2001) is important for the model to predict AN fiber temporal response properties (e.g., synchronization index) across levels.

The V_{IHC}-k (or V_{IHC}-P_I) relationship for model AN fibers should also be characteristic frequency (CF) dependent. The voltage responses of the IHC at various basilar-membrane locations to a tone at CF have different ac/dc components (Cheatham and Dallos, 1993),[2] and attenuation of the AC component at high frequencies suggests that a steeper slope of V_{IHC}-k relationship (or V_{IHC}-P_I, see Zhang *et al.*, 2001) is required to generate similar rate-level functions.

Physiologically, the transmitter release at the IHC-AN synapse is controlled through V_{IHC}-dependent calcium dynamics, and is highly nonlinear and complex. Calcium dynamics have been considered in recent versions of these models. Sumner *et al.* (2002) included a specific calcium-controlled transmitter-release function in the Meddis model, and Zhang *et al.* (2001) used low-pass filters and an *ad hoc* control function to model the effects of calcium dynamics.

E. Understanding the relationship between offset and onset adaptation

The study shows that a simple shift can improve the model's offset adaptation without compromising the model's onset adaptation characteristics. Inclusion of offset adaptation in the model improves the model's prediction of the temporal aspects of the AN fiber responses and thus benefits other modeling studies based on the temporal responses of AN fibers (e.g., modulation studies). A negative adaptation was used in a previous study (Ross, 1996) to produce the deadtime period in the offset adaptation. This negative adaptation was limited to one of the parallel pathways and thus had a limited contribution to the temporal responses of AN fibers. The physiological meaning of the negative adaptation also needs further explanation.

The shift A_{shift} introduced in the present model can be

interpreted as a constant threshold (either concentration or number of neurotransmitter molecules) in the synaptic cleft before the transmitter reaches the postsynaptic site. When the transmitter concentration in the cleft is higher than A_{shift}, the firing probability in the postsynaptic neuron changes linearly as a function of concentration. The firing probability in the postsynaptic neuron approaches zero quickly when the transmitter concentration is less than A_{shift} (so zero in the model output could be interpreted as a very low firing probability). Since the offset adaptation of the AN fiber is related to the spontaneous rate (Harris and Dallos, 1979; Westerman, 1985), it is reasonable for the value of the shift to vary as a function of the spontaneous rate of the fiber as well. Further study of how the value of the shift is related to the other characteristics of the model fiber responses is needed.

Also, the results show that the offset adaptation time constant is closely related to the short-term constant of the onset adaptation for the model explored. In fact, if the model onset adaptation is measured from level L_0 to level L_1 (L_0 is the level before the onset and L_1 is the level after onset) and offset adaptation is measured from level L_2 to L_1 (L_2 is the level before the offset and L_1 is the level after the offset), the time constants for the onset short-term component and for the offset adaptation are the same, based on Eq. (17). Whether this is a limitation of the model or reflects some underlying mechanism of the synapse requires further examination.

Our modification to improve the model's offset adaptation is based on the assumed shape of offset adaptation from physiological studies: A period of deadtime (or period of low firing probability), followed by a single slow recovery function. Whether other characteristic functions can provide a better fit for the physiological data is an interesting topic for future studies. The modification of the model will be further justified if future studies suggest that this characteristic function provides a better fit to the physiological data than that of other models.

F. Extension of analytical approach to other models

The mathematical methods proposed in this study are also useful for analysis of models with other structures. Several models (Smith and Brachman, 1982; Ross, 1996) include parallel pathways of transmitter reservoirs to produce the additivity of responses to increments. These models could also be described by differential equations, and the relationship between adaptation characteristics and model parameters can be established for further understanding of these models.

The analytical approach provided in this study can help us to identify the candidate model that represents the actual underlying physiological mechanism. Values of model parameters can be derived from our analytical approach for different amounts of adaptation in the IHC-AN synapse, due to either different IHC-AN synapses (i.e., different AN fiber types) or to different stimulus levels. By studying the physiological changes of the synapse with different amounts of adaptation, and the correlation between changes of the model parameters and physiological properties, we can validate if the model can represent the actual physiological mechanism. For example, physiological studies (Moser and Beutner, 2000) support the idea that rapid adaptation is due to the depletion of the synapse material in the immediate store that is present in both models considered here.

Modeling the IHC-AN synapse is still a very challenging task because of the synapse structure (how the reservoirs are connected) and the processing dynamics (how the V_{IHC} affects model parameters such as permeabilities). While it is easy to complicate the IHC-AN synapse model with more physiologically realistic structures, the benefit of such complications in providing more accurate responses should be carefully studied. Modeling studies of other adaptation measures (Hewitt and Meddis, 1991; Sumner *et al.*, 2002, 2003), which focused on models with preset parameters, should also be extended. An analysis of the relationship of these adaptation measures and how they are affected by the model parameters will greatly improve our knowledge of both IHC-AN synapse models and of the underlying physical system.

ACKNOWLEDGMENTS

This work was supported by NIH-NIDCD Grant No. R01-01641. We gratefully acknowledge the comments of Dr. Robert Smith on a previous version of this manuscript, and the editorial assistance of Susan Early.

APPENDIX: RELATIONSHIP BETWEEN ADAPTATION CHARACTERISTICS AND THE MEDDIS-MODEL PARAMETERS

The Meddis model with three neurotransmitter reservoirs (q,w,c) can be described by the simplified Eqs. (A1) and (A2) [rewritten from Eqs. (14) and (15)]:

$$\frac{dq}{dt} = y(M - q(t)) - kq(t) + xw(t), \tag{A1}$$

$$\frac{dw}{dt} = kuq(t) - xw(t). \tag{A2}$$

The model parameters M, y, x, u are constant, and k is the level-dependent permeability, which is denoted as k_1 before the onset and as k_2 after the onset.

The onset adaptation of the model synapse is characterized by:

$$R_{\text{on}}(t) = A_{\text{sus}} + A_r e^{-t/\tau_R} + A_{\text{st}} e^{-t/\tau_{\text{ST}}}, \tag{A3}$$

with a spontaneous rate of A_{sp}, where A_{sus}, A_r, and A_{st} represent the response amplitude (instantaneous firing rate) of the sustained component, rapid adaptation component, and short-term adaptation component, and τ_R and τ_{ST} represent the time constants of the rapid and short-term adaptation components.

If we assume that $kq(t)$ is the output of the model synapse, the relationship between the model parameters and adaptation characteristics can be described by the following equations [$-1/\tau_R$ and $-1/\tau_{\text{ST}}$ are the poles of $Q(s)$ in Eq. (17)]:

$$\frac{k_1}{k_2} = \frac{A_{sp}}{A_r + A_{st} + A_{sus}}, \tag{A4}$$

$$\frac{yMk_1}{y + k_1(1-u)} = A_{sp}, \tag{A5}$$

$$\frac{yMk_2}{y + k_2(1-u)} = A_{sus}, \tag{A6}$$

$$x + k_2 + y = 1/\tau_R + 1/\tau_{ST}, \tag{A7}$$

$$x(y + k_2(1-u)) = 1/(\tau_R \tau_{ST}), \tag{A8}$$

$$\frac{k_2}{k_1}(k_2 - k_1)A_{sp} = A_r/\tau_R + A_{sus}/\tau_{ST}. \tag{A9}$$

Several intermediate parameters are useful for the derivation of the model parameters:

$$A_{on} = A_{sus} + A_r + A_{st}, \tag{A10}$$

$$S_r = 1/\tau_R + 1/\tau_{ST} \tag{A11}$$

$$S_{r2} = A_r/\tau_R + A_{st}/\tau_{ST}, \tag{A12}$$

$$P_r = 1/(\tau_R \tau_{ST}). \tag{A13}$$

From Eqs. (A4) and (A9), k_1 and k_2 can be specified as:

$$k_2 = S_{r2}/(A_{on} - A_{sp}), \quad k_1 = A_{sp}/A_{on}k_2. \tag{A14}$$

Several other intermediate parameters are defined as:

$$\beta = (A_{sus} - A_{sp})k_1 k_2/(A_{sp}k_2 - A_{sus}k_1), \tag{A15}$$

$$a = (\beta + k_2)\beta, \quad b = -(S_r - k_2)(\beta + k_2), \quad c = P_r, \tag{A16}$$

$$z = -\frac{-b + \sqrt{b^2 - 4ac}}{2a}. \tag{A17}$$

The other model parameters then are set as follows:

$$u = 1 - z, \tag{A18}$$

$$y = \beta z, \tag{A19}$$

$$x = S_r - k_2 - y, \tag{A20}$$

$$M = \frac{A_{sp}(y + k_1 z)}{yk_1}. \tag{A21}$$

Computer code related to the material in this Appendix is available at the website http://web.syr.edu/~lacarney/.

[1]The model results presented here are illustrative. More extensive explorations have been conducted in another study (Nelson and Carney, 2004).

[2]We (and others) have assumed that there is no adaptation in the voltage responses of the IHC, but a recent study suggests that there may indeed be some adaptation at this level. It is important to explore the contribution of the IHC adaptation described by Zeddies and Siegel (2004) to AN responses, especially at the onset and offset of tone bursts and in response to AM stimuli.

Carney, L. H. (**1993**). "A model for the responses of low-frequency auditory-nerve fibers in cat," J. Acoust. Soc. Am. **93**(1), 401–417.

Cheatham, M. A., and Dallos, P. (**1993**). "Longitudinal comparisons of IHC ac and dc receptor potentials recorded from the guinea pig cochlea," Hear. Res. **68**(1), 107–114.

Furukawa, T., and Matsuura, S. (**1978**). "Adaptive rundown of excitatory postsynaptic potentials at synapses between hair cells and eight nerve fibers in the goldfish," J. Physiol. (London) **276**, 193–209.

Harris, D. M., and Dallos, P. (**1979**). "Forward masking of auditory nerve fiber responses," J. Neurophysiol. **42**(4), 1083–1107.

Heinz, M. G., Zhang, X., Bruce, I. C., and Carney, L. H. (**2001**). "Auditory-nerve model for predicting performance limits of normal and impaired listeners," ARLO **2**, 91–96.

Hewitt, M. J., and Meddis, R. (**1991**). "An evaluation of eight computer models of mammalian inner hair-cell function," J. Acoust. Soc. Am. **90**(2 Pt 1), 904–917.

Joris, P. X., and Yin, T. C. (**1992**). "Responses to amplitude-modulated tones in the auditory nerve of the cat," J. Acoust. Soc. Am. **91**(1), 215–232.

Meddis, R. (**1986**). "Simulation of mechanical to neural transduction in the auditory receptor," J. Acoust. Soc. Am. **79**(3), 702–711.

Meddis, R. (**1988**). "Simulation of auditory-neural transduction: Further studies," J. Acoust. Soc. Am. **83**(3), 1056–1063.

Meddis, R., Hewitt, M. J., and Shackleton, T. (**1990**). "Implementation details of a computational model of the inner hair-cell/auditory-nerve synapse," J. Acoust. Soc. Am. **87**, 1813–1818.

Moser, T., and Beutner, D. (**2000**). "Kinetics of exocytosis and endocytosis at the cochlear inner hair cell afferent synapse of the mouse," Proc. Natl. Acad. Sci. U.S.A. **97**(2), 883–888.

Nelson, P., and Carney, L. (**2004**). "A phenomenological model of peripheral and central neural responses to amplitude-modulated tones," J. Acoust. Soc. Am. **116**, 2173–2186.

Raman, I. M., Zhang, S., and Trussell, L. O. (**1994**). "Pathway-specific variants of AMPA receptors and their contribution to neuronal signaling," J. Neurosci. **14**(8), 4998–5010.

Relkin, E. M., and Doucet, J. R. (**1991**). "Recovery from prior stimulation. I: Relationship to spontaneous firing rates of primary auditory neurons," Hear. Res. **55**(2), 215–222.

Rhode, W. S., and Smith, P. H. (**1985**). "Characteristics of tone-pip response patterns in relationship to spontaneous rate in cat auditory nerve fibers," Hear. Res. **18**(2), 159–168.

Ross, S. (**1996**). "A functional model of the hair cell-primary fiber complex," J. Acoust. Soc. Am. **99**(4 Pt 1), 2221–2238.

Russell, I. J., and Sellick, P. M. (**1978**). "Intracellular studies of hair cells in the mammalian cochlea," J. Physiol. (London) **284**, 261–290.

Schwid, H. A., and Geisler, C. D. (**1982**). "Multiple reservoir model of neurotransmitter release by a cochlear inner hair cell," J. Acoust. Soc. Am. **72**(5), 1435–1440.

Smith, R. L., and Zwislocki, J. J. (**1975**). "Short-term adaptation and incremental responses of single auditory-nerve fibers," Biol. Cybern. **17**(3), 169–182.

Smith, R. L. (**1977**). "Short-term adaptation in single auditory nerve fibers: Some poststimulatory effects," J. Neurophysiol. **40**(5), 1098–1111.

Smith, R. L., and Brachman, M. L. (**1982**). "Adaptation in auditory-nerve fibers: A revised model," Biol. Cybern. **44**(2), 107–120.

Smith, R. L., Brachman, M. L., and Frisina, R. D. (**1985**). "Sensitivity of auditory-nerve fibers to changes in intensity: A dichotomy between decrements and increments," J. Acoust. Soc. Am. **78**(4), 1310–1316.

Sumner, C. J., Lopez-Poveda, E. A., O'Mard, L. P., and Meddis, R. (**2002**). "A revised model of the inner-hair cell and auditory-nerve complex," J. Acoust. Soc. Am. **111**(5 Pt 1), 2178–2188.

Sumner, C. J., Lopez-Poveda, E. A., O'Mard, L. P., and Meddis, R. (**2003**). "Adaptation in a revised inner-hair cell model," J. Acoust. Soc. Am. **113**(2), 893–901.

Westerman, L. A., and Smith, R. L. (**1984**). "Rapid and short-term adaptation in auditory nerve responses," Hear. Res. **15**(3), 249–260.

Westerman, L. A. (**1985**). *Adaptation and recovery of auditory nerve responses*, Institute for Sensory Research, Syracuse Univ., Syracuse, N.Y.

Westerman, L. A., and Smith, R. L. (**1988**). "A diffusion model of the transient response of the cochlear inner hair cell synapse," J. Acoust. Soc. Am. **83**(6), 2266–2276.

Zeddies, D. G., and Siegel, J. H. (**2004**). "A biophysical model of an inner hair cell," J. Acoust. Soc. Am. **116**(1), 426–441.

Zhang, X., Heinz, M. G., Bruce, I. C., and Carney, L. H. (**2001**). "A phenomenological model for the responses of auditory-nerve fibers. I: Nonlinear tuning with compression and suppression," J. Acoust. Soc. Am. **109**(2), 648–670.